AIMS Materials Science, 4(6): 1220-1230.
DOI: 10.3934/matersci.2017.6.1220
Received: 29 September 2017
Accepted: 21 November 2017
Published: 23 November 2017

http://www.aimspress.com/journal/Materials

Research article

Human bone ingrowth into a porous tantalum acetabular cup

Gregory N. Haidemenopoulos [1,2,*], Kostantinos N. Malizos [3], Anna D. Zervaki [1], and Kostantinos Bargiotas [3]

[1] Department of Mechanical Engineering, University of Thessaly, Volos, Greece
[2] Department of Mechanical Engineering, Khalifa University of Science and Technology, Abu Dhabi, UAE
[3] Department of Orthopedics, Faculty of Medicine, University of Thessaly, Larissa, Greece

*** Correspondence:** Email: grigorios.chaidemenopoulos@kustar.ac.ae; Tel: +971506583867.

Abstract: Porous Tantalum is increasingly used as a structural scaffold in orthopaedic applications. Information on the mechanisms of human bone ingrowth into trabecular metal implants is rather limited. In this work we have studied, qualitatively, human bone ingrowth into a retrieved porous tantalum monoblock acetabular cup using optical microscopy, scanning electron microscopy and energy dispersive X-ray analysis. According to the results and taking into account the short operational life (4 years) of the implant, bone ingrowth on the acetabular cup took place in the first two-rows of porous tantalum cells to an estimated depth of 1.5 to 2 mm. The bone material, grown inside the first raw of cells, had almost identical composition with the attached bone on the cup surface, as verified by the same Ca:P ratio. Bone ingrowth has been a gradual process starting with Ca deposition on the tantalum struts, followed by bone formation into the tantalum cells, with gradual densification of the bone tissue into hydroxyapatite. A critical step in this process has been the attachment of bone material to the tantalum struts following the topology of the porous tantalum scaffold. These results provide insight to the human bone ingrowth process into porous tantalum implants.

Keywords: porous tantalum; bone ingrowth; acetabular cup; osteointegration; tantalum scaffold

1. Introduction

New highly porous metals have been developed in the recent years for use in orthopedic surgery, including porous titanium and porous tantalum in the form of coating or bulk metallic foams. Porous

coated implants have been successfully used in joint replacement surgery [1,2]. As an example, laser-deposited tantalum coatings on titanium implants have been studied as potential replacement of hydroxyapatite coatings [3]. Experimental studies, autopsy of retrieved implants and long term clinical results have confirmed that bone ingrowth does occur and in most cases creates a mechanically sufficient interface that provides long standing implant incorporation. On the other hand, micromotion, implant migration and penetration of microparticles into the interface do occur resulting in osteolysis and implant failure [4,5]. Several additional limitations, such as low porosity and relatively high Young's modulus, led to the introduction of metallic foams as candidate biomaterials for total hip arthroplasty and other orthopedic applications. Levine has reviewed the basic characteristics and biomaterials properties of these materials in orthopedic applications [6]. It appears that these materials satisfy the basic requirements related to their use as scaffold materials for reconstruction of bone [7]. The most important of these developments has been the porous tantalum biomaterial. The material exhibits an open cell structure of repeated dodecahedrons. It is produced by chemical vapor infiltration (CVI) of commercially pure tantalum onto a vitreous carbon scaffolding. The fabrication methods and relevant biomaterial properties of porous tantalum, including high porosity and low modulus of elasticity, have been recently reviewed by Chen et al. [8]. In addition Mediaswanti et al. [9] as well as Cristea et al. [10] have shown that bioperformance, including pore filling and osteointegration, are influenced by pore size and surface roughness of porous tantalum. The bone ingrowth performance of this material has been addressed in the well-known experimental studies by Bobyn et al. in transcortical canine model [11,12]. However the human bone ingrowth characteristics have received less attention due to the difficulties of obtaining human specimens. Therefore the assessment of bone to implant fixation and osteointegration has been mostly based on radiological and clinical studies [13–16]. Only recently D'Angelo et al. performed a histological evaluation of bone-implant interface in a human specimen removed from a patient, using polarized light microscopy, to evaluate the degree of pore filling by bone [17]. In addition Hanzlik et al. performed studies of human bone ingrowth in retrieved porous tantalum components and compared the ingrowth process in modular and monoblock designs [18,19].

In the present work, we studied human bone in-growth into a retrieved porous tantalum monoblock acetabular cup using optical microscopy, scanning electron microscopy and energy dispersive X-ray analysis in an effort to evaluate the characteristics and mechanisms of human bone in-growth including the depth of bone ingrowth, the degree of cell filling and bone attachment to the porous tantalum struts.

2. Materials and Methods

2.1. Implantation Details

A 42-year female patient with advanced post-traumatic hip osteoarthritis underwent total hip replacement with a monoblock porous tantalum—trabecular metal elliptical cup (Zimmer Warsow, Indiana). The patient developed hip instability with multiple episodes of hip dislocations over a period of three years post-operatively. Although radiologically stable, the cup was removed at 4 years post-implantation in order to address hip instability. The cup was retrieved through a standard posterior approach with the specially designed instrument provided by the manufacturer. This allowed implant removal with minor acetabular damage. Marginal removal of the attached bone took

place. After removal the cup was cleaned with normal saline, foreign bodies and debris was removed and it was stored in a sterile package. Consent has been granted by the patient for this study. It is anticipated that this is not a standard implant, since its operational life was only 4 years while the patient is not a typical THA-patient due to the young age. However it was considered that, due to the short operational life, it would serve to study the early stages of osteointegration.

2.2. Specimen Preparation

The acetabular cup is shown, after removal, in Figure 1. There are areas with visible bone still attached on the surface as well as areas that are bone-free. The curved lines in Figure 1 indicate the two transverse cuts, that were performed through the acetabular cup using a thin SiC cutting disc in an Acutom cutting machine (Struers, Denmark). A low cutting speed and water cooling were employed during cutting. Three specimens were taken, Specimen 1 from a region with no visible bone attachment and Specimens 2 and 3 from regions with visible bone attachments.

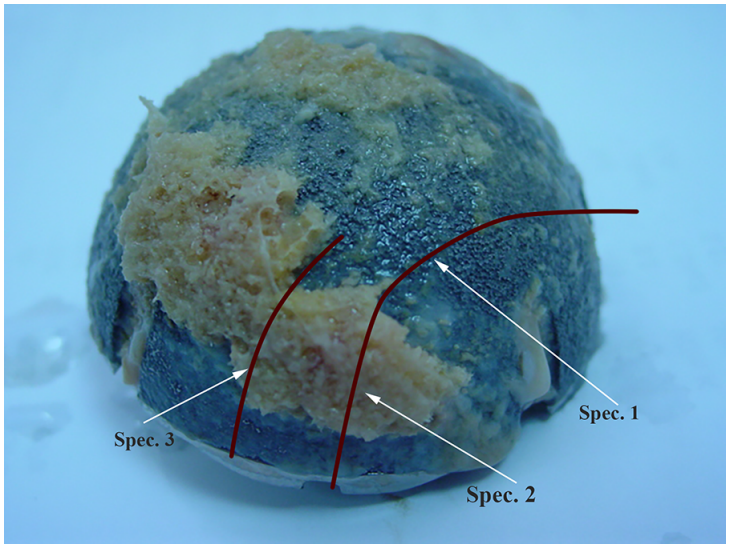

Figure 1. Porous tantalum acetabular cup with visible bone attachments. The lines indicate the cutting trajectories and position of specimens.

The specimens for optical microscopy were prepared by employing the standard metallographic mounting, grinding and polishing techniques. Mounting was performed in Epofix resin (Struers, Denmark) using 30 mm diameter molds. Grinding was performed on a Knuth-Rotor 3 (Struers, Denmark) grinding machine using 600 and 1000 grit SiC papers and cooling with water. Polishing was performed in three steps in a DAP-V (Struers, Denmark) polishing machine. In the first step, a polishing clothe and diamond paste with 3 μm grain diameter was used. In the second step, a diamond paste with 1 μm grain diameter was used. Finally, in the third step, an alumina slurry was used as a polishing compound. Between the polishing steps the specimens were cleaned with alcohol. Finally, after polishing, the specimens were cleaned and dried in warm air.

2.3. Microscopy—Microanalysis

Examination of the transverse sections was performed in an Aristomet metallographic microscope (Leitz, Germany). Examination of the surface of the acetabular cup was performed in a WILD M3Z stereo microscope (Leica, Germany). Examination of the cup surface as well as the transverse sections was performed in a JEOL JSM-62100 SEM (JEOL, Japan) equipped with an Energy dispersive spectroscopy (EDS) detector. Prior to observation the specimens were gold-coated in order to reduce charging effects.

3. Results and Discussion

3.1. Specimen 1—No Visible Bone Attachment

As seen in Figure 1, Specimen 1 was taken from a region with no visible bone attachment on the cup's surface. The structure of the porous tantalum scaffold, as revealed by SEM, is shown in Figure 2(a) with the composite struts consisting of the vitreous carbon skeleton and tantalum chemical vapor infiltration (CVI) deposit. Cell size ranged between 400 and 600 μm while the tantalum deposit thickness ranged between 40 and 60 μm. The average volume porosity of the scaffold was estimated to be 80%. The above values are very close to those reported by Levine et al. [20]. The fine structure of the strut's surface is shown in Figure 2(b). Due to the crystalline nature of the tantalum deposit, the surface is faceted. This could facilitate the attachment of new bone to the surface of the struts. The grain size ranged between 2 and 10 μm while the mean grain size was 6 μm. Examination of the surface of the transverse section of Specimen 1 (metallographic sample) in Figure 3 shows that the tantalum/carbon interface is relatively smooth while the surface of the tantalum deposit is relatively rough due to its faceted nature.

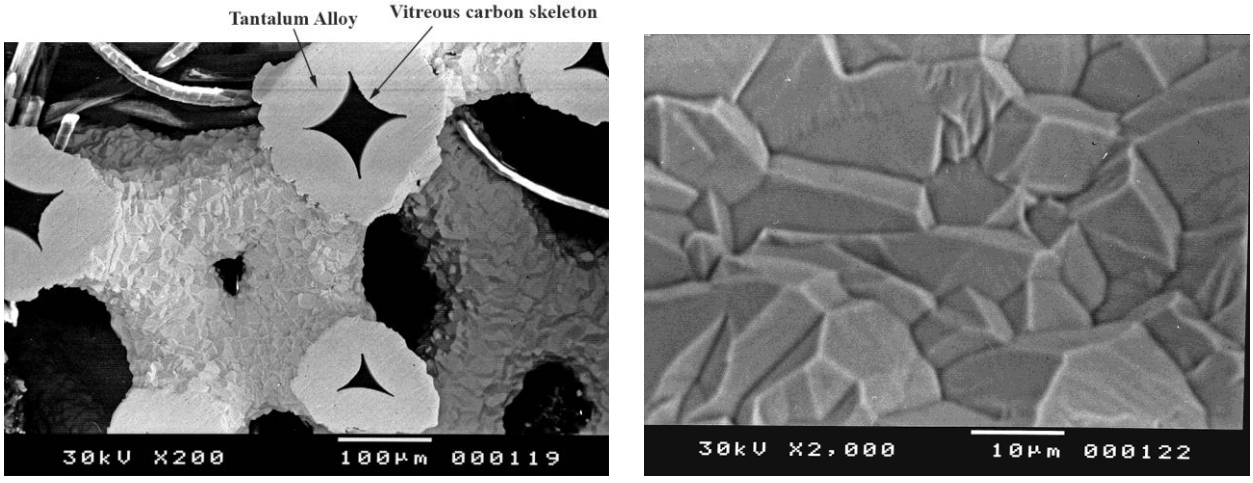

(a) (b)

Figure 2. (a) Backscattered SEM image of the porous tantalum scaffold showing the vitreous carbon skeleton, (b) faceted surface of tantalum struts.

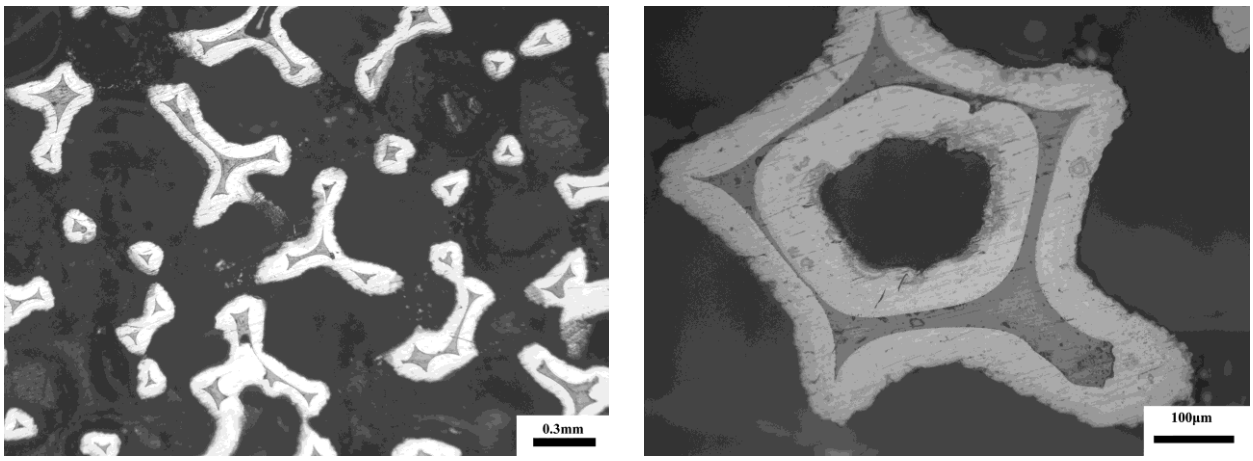

(a) (b)

Figure 3. (a) Metallographic transverse section of Specimen 1, (b) a higher magnification image showing the smooth tantalum/carbon interface and rough tantalum deposit surface.

3.2. Specimens 2 and 3—Visible Bone Attachment

A transverse metallographic section of Specimen 2 indicating bone ingrowth in the first two series of cells is depicted in Figure 4. EDS spectrum of bone reveals calcium (Ca), phosphorous (P) and oxygen (O) as expected. Composition is 28.16 carbon, 51.31 oxygen, 7.29 phosphorous and 13.14 calcium (in mol%). The Ca:P ratio is 1.77, very close to the value 1.66 for hydroxyapatite. A magnification of the encircled region in Figure 4(a) is shown in Figure 4(b) with the respective EDS spectrum. The bone has filled completely the cell and has entered the second cell bellow. The EDS spectrum corresponds to a composition of 32.32 carbon, 47.37 oxygen, 7.16 phosphorous and 12.12 Ca (in mol%), with a Ca:P ratio equal to 1.69, which is very close to 1.66 for hydroxyapatite, indicating a complete densification into hydroxyapatite. Examination of the bone-implant interface indicates that there are regions where the bone is fully attached to the strut surface and regions where the attachment is less coherent.

An additional transverse section of Specimen 2 is shown in Figure 5. Attention should be paid in Figure 5(b) which is an EDS mapping of calcium (red dots) and tantalum (green dots). The map shows the regions of high concentration of calcium, indicating the ingrowth of bone into the cells of the implant. Figure 6 shows a metallographic transverse section of a region 0.5 to 1 mm below the surface of the implant and associated EDS maps of calcium in Figure 6(b)—red dots, tantalum in Figure 6(b)—green dots, phosphorous in Figure 6(c) and carbon in Figure 6(d). Again high concentration of calcium and phosphorous indicates bone formation in the tantalum cells. Calcium was also detected on the surface of the struts in regions 1 mm below the surface of the implant were no visible bone formation exists.

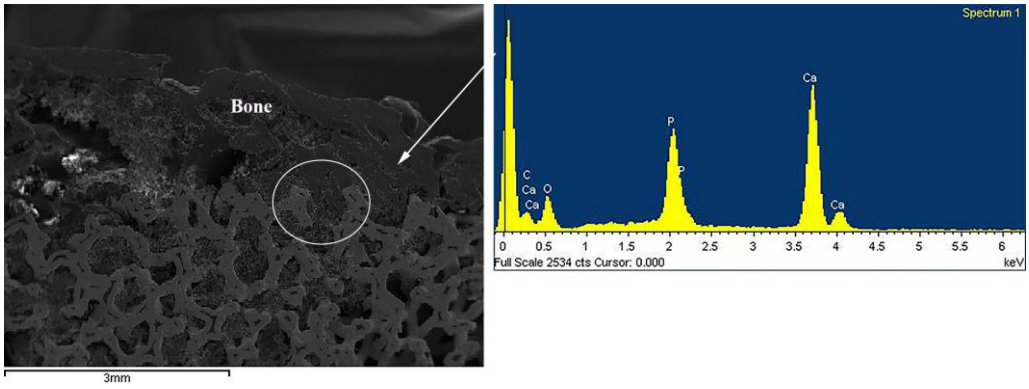

(a)

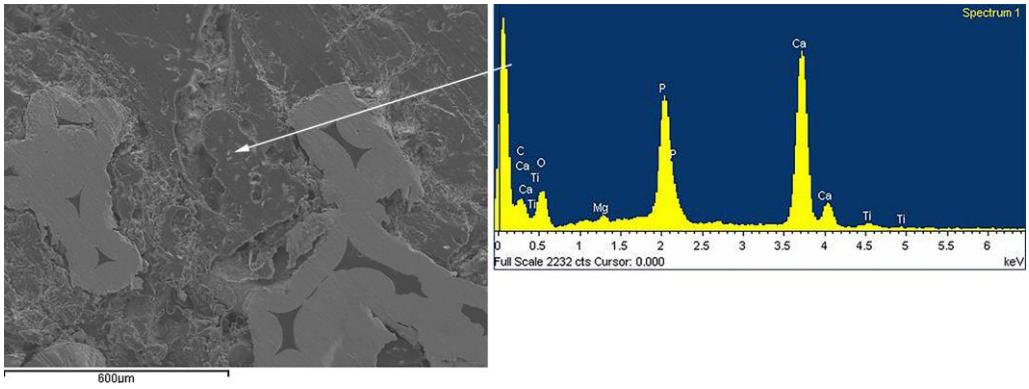

(b)

Figure 4. (a) Metallographic transverse section of Specimen 1 indicating bone attachment and ingrowth, (b) area encircled in (a) with bone ingrowth in the first open cell. Respective EDS spectra are also shown.

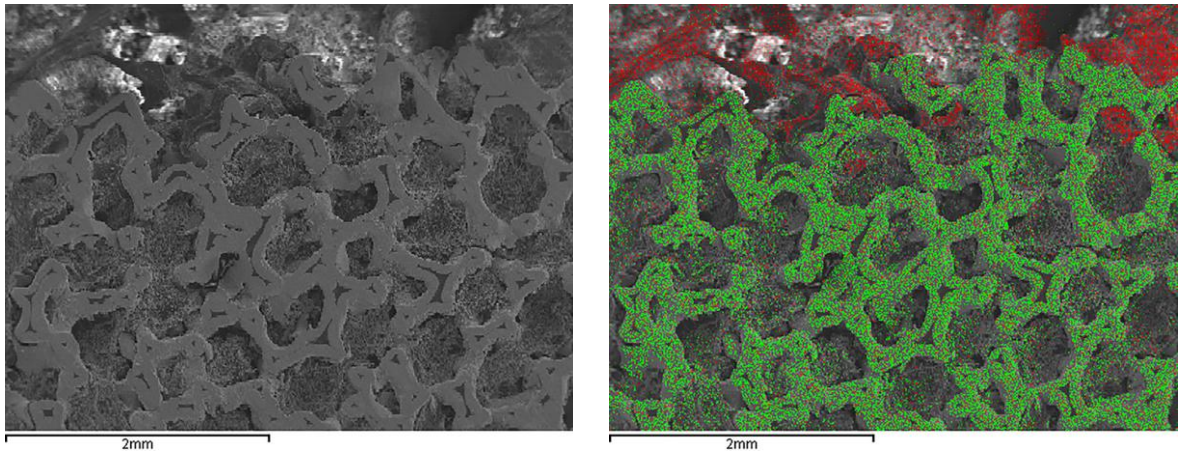

(a) (b)

Figure 5. (a) Metallographic section of Specimen 2 showing bone attachment and ingrowth in the porous tantalum implant (b) X-ray map of Ca (red dots) and tantalum (green dots).

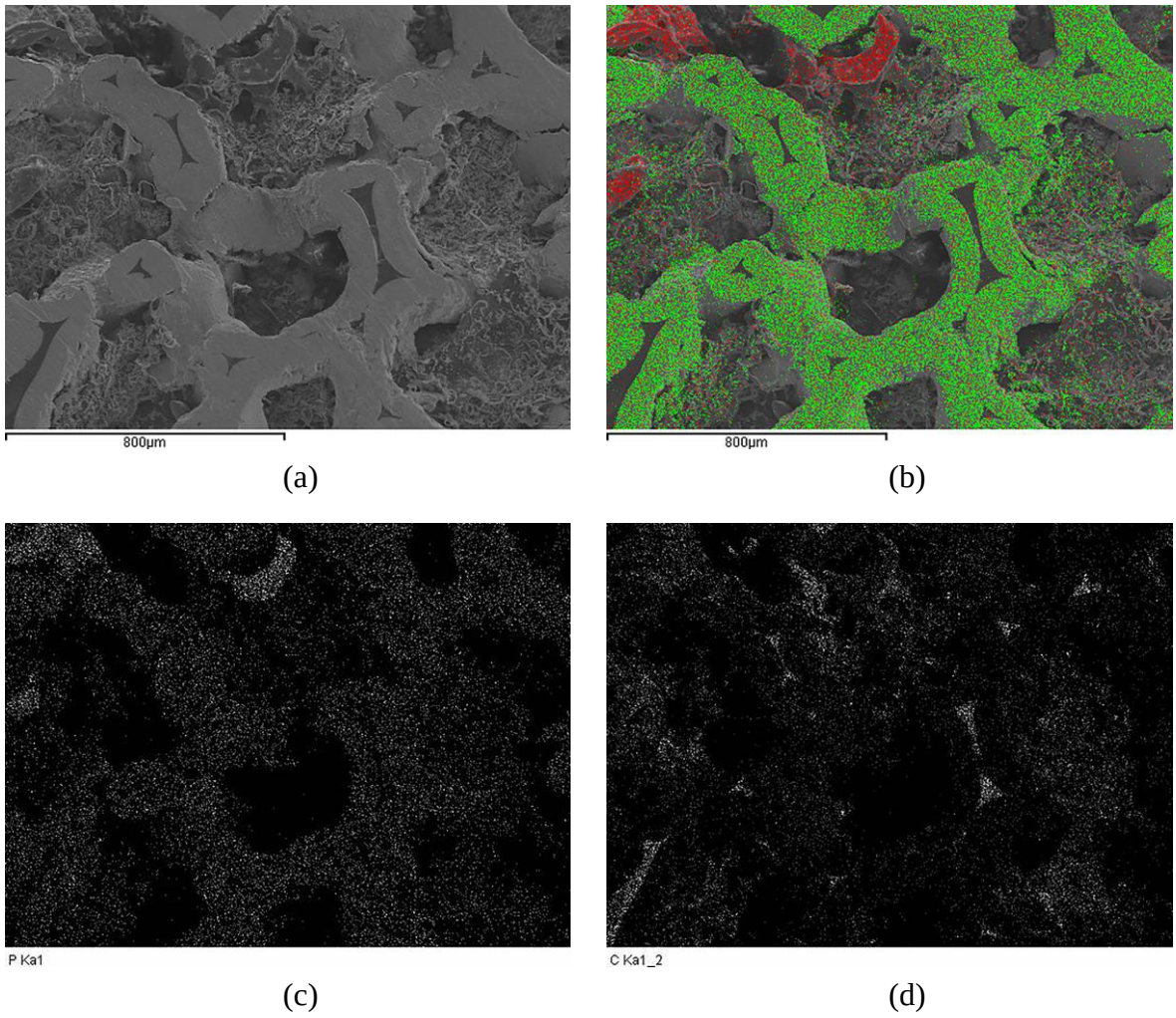

Figure 6. (a) Transverse metallographic section of Specimen 2 at 0.5–1.0 mm depth from the bone-implant interface, (b) calcium (red dots) and tantalum (green dots) EDS map, (c) phosphorous EDS map, (d) carbon EDS map.

Specimen 3 was cut from a region where the attached bone was thicker as a result of the cup removal process. A metallographic section of Specimen 3 is shown in Figure 7 indicating three regions: the attached cancellous bone, the bone-implant interface and the region of bone ingrowth into the tantalum cell structure. The bone ingrowth region extends up to 1.5 mm depth from the bone-implant interface, in agreement with experimental data [11,17,18]. The lower-right area of this region is shown in higher magnification in Figure 8. EDS spectra from regions A and B are also shown in Figure 8. Composition of region A is carbon 44.50, oxygen 38.32, phosphorous 5.85, calcium 10.53 (in mol%). At region A, there is formation of new bone in the first open cell of the porous tantalum scaffold as indicated by the presence of Ca, P and O. At region B, the cell is filled with what appears to be bone material. The composition from the EDS signal is carbon 80.38, oxygen 15.79, calcium 3.69 (in mol%). It appears that EDS revealed the presence of calcium but no presence of phosphorous. It is known that ingrowth occurs with a healing cascade that resembles healing of a cancellous defect. Intramembranous ossification occurs as soon as the first week and woven bone formation is seen in and around the pores within 3 weeks. Lamellar bone remodelling follows, replacing woven bone by structured lacunae. Although it is unclear to what extent this

process might occur, vascularisation and oxygen supply play a key role to the advancement of the haversian remodeling.

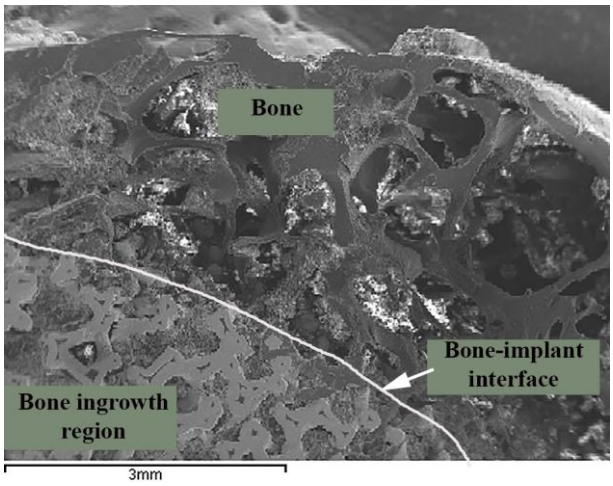

Figure 7. Transverse metallographic section of Specimen 3 showing attached bone, the bone-implant interface and the region of bone ingrowth.

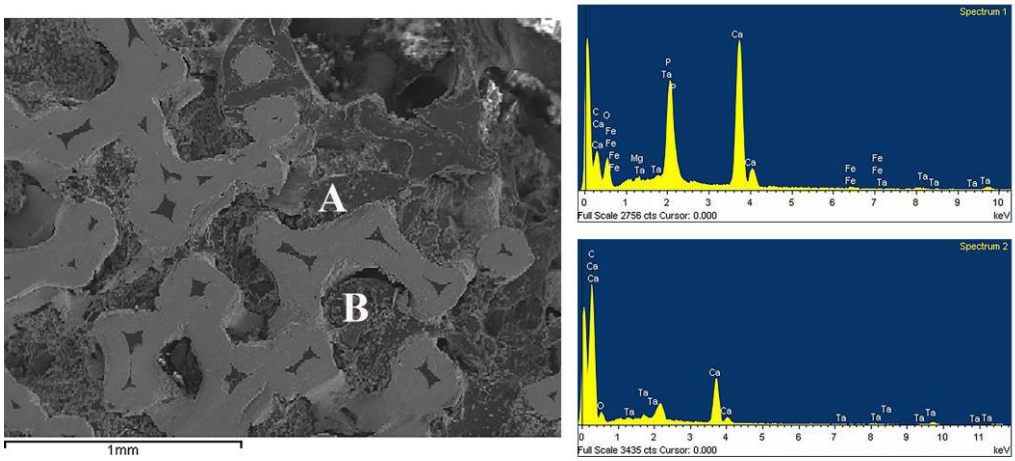

Figure 8. Higher magnification of bone ingrowth region of Figure 7 with EDS spectrum of regions A and B.

The morphology of bone ingrowth is depicted in Figure 9, which is a transverse metallographic section of Specimen 3. At first, bone fills the open cells of the tantalum scaffold (e.g., regions A and B) and then proceeds to fill cells deeper in the scaffold (e.g., region C). In order to fill an empty cell, bone is attached on the tantalum struts surrounding the cell (e.g., points 1 and 2) and fills the empty space by further growth of hydroxyapatite crystals. The macroscopic observation is, therefore, that bone ingrowth starts with bone filling the first row of open cells on the porous tantalum cup surface and proceeds with the filling of the second row of cells. These results indicate that bone ingrowth into porous tantalum is partial, in agreement with observations in the work of Hanzlik et al. [19].

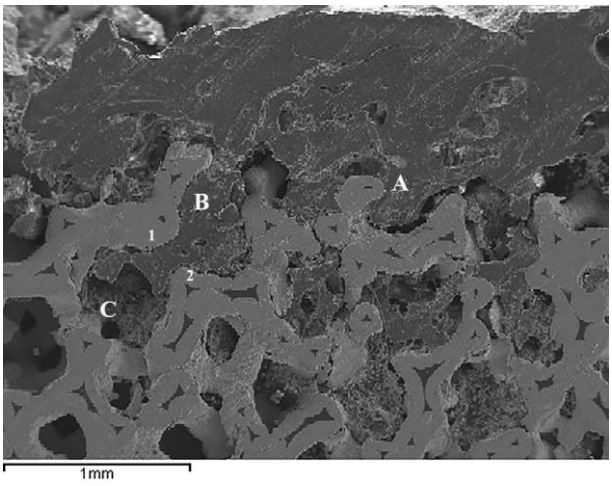

Figure 9. Transverse metallographic section of Specimen 3 showing attached bone and the region of bone ingrowth. Bone ingrowth into open cells is shown in A and B while ingrowth into cells deeper in the tantalum scaffold is shown at C.

During ingrowth, bone follows the topology of the scaffold by attaching on the tantalum struts and then fills the empty space of the cells. It has been suggested that a self-passivating surface oxide layer leads to the formation of a bone-like apatite coating in vivo facilitating bone attachment [20]. In addition, in a recent work by Paganias et al., it was shown that hydroxyapatite-like coating could be formed on the porous tantalum surface when treated with NaOH solution [21,22]. When impregnated into simulated body fluid, the treated surface indicated hydroxyapatite formation in one week. This could explain the good integration characteristics of porous tantalum implants. Limitations of this work are related to the following issues: (a) the study was based on a single implant, and (b) the implant was retrieved from a relatively young, at the time of removal, patient. It is anticipated that bone ingrowth is inferior in cases of elderly, osteoporotic patients, which make up the majority of patients undergoing surgery for total hip arthroplasty. Further retrieval studies are, therefore, mandatory in order to fully understand the process of bone ingrowth into porous tantalum and its clinical relevance.

4. Conclusion

According to the results presented above and taking into account the short operational life of the implant, bone ingrowth on the acetabular cup occurs in the first two-rows of porous tantalum cells to an estimated depth of 1.5 to 2 mm. The bone material, grown inside the first raw of cells, had almost identical composition with the attached bone on the cup surface, as verified by the same Ca:P ratio. For the present case, it appears that bone ingrowth has been a gradual process starting with Ca deposition on the tantalum struts, followed by bone formation into the tantalum cells, with gradual densification of the bone tissue into hydroxyapatite. A critical step in this process has been the attachment of bone material to the tantalum struts following the topology of the porous tantalum scaffold.

Acknowledgments

This research received no specific grant from any funding agency in the public, commercial, or not-for-profit sectors.

Conflict of Interest

The authors declare that there is no conflict of interest regarding the publication of this manuscript.

References

1. Engh CA, Hopper RH, Engh CA (2004) Long-term porous-coated survivorship using spikes, screws and press fitting for initial fixation. *J Arthroplasty* 19: 54–60.
2. Engh CA, Zettl-Schaffer KF, Kukita Y, et al. (1993) Histological and radiographic assessment of well-functioning porous-coated acetabular componenents. A human postmortem retrieval study. *J Bone Joint Surg Am* 75: 814–824.
3. Roy M, Balla VK, Bose S, et al. (2010) Comparison of tantalum and hydroxyapatite coatings on tantalum for applications in load bearing implants. *Adv Eng Mater* 12: B637–B641.
4. Udomkiat P, Dorr LD, Wan Z (2002) Cementless hemispheric porous-coated sockets implanted with press-fit technique without screws: average ten-year follow up. *J Bone Joint Surg Am* 84: 1195–1200.
5. Pidhorz LE, Urban RM, Jacobs JJ (1993) A quantitative study of bone and soft tissues in cementless porous-coated acetabular components retrieved at autopsy. *J Arthroplasty* 8: 213–225.
6. Levine B (2008) A new era in porous metals: applications in orthopedics. *Adv Eng Mater* 10: 788–792.
7. Eisenbarth E (2007) Biomaterials for tissue engineering. *Adv Eng Mater* 9: 1051–1060.
8. Chen CJ, Zhang M (2012) Fabrication methods of porous tantalum metal implants for use as biomaterials. *Adv Mater Res* 476–478: 2063–2066.
9. Mediaswanti K, Wen C, Ivanova EC, et al. (2013) A review on bioactive porous metallic biomaterials. *J Biomim Biomater Tissue Eng* 18: 1–8.
10. Cristea D, Ghiuta I, Muntenau D (2015) Tantalum based materials for implants and prostheses applications. *B Transilvania Univ Brasov Eng Sci Ser I* 8: 151–158.
11. Bobyn JD, Stackpool G, Hacking SA, et al. (1999) Characteristics of bone ingrowth and interface mechanics of a new porous tantalum biomaterial. *J Bone Joint Surg Br* 81: 907–914.
12. Bobyn JD, Toh KK, Hacking SA, et al. (1999) Tissue response to porous tantalum acetabular cups: a canine model. *J Arthroplasty* 14: 347–354.
13. Malizos KN, Bargiotas K, Papatheodorou L, et al. (2008) Survivorship of monoblock trabecular metal cups on primary THA: midterm results. *Clin Orthop Relat R* 466: 159–166.
14. Xenakis T, Macheras G, Stafilas K, et al. (2009) Multicenter use of a porous tantalum monoblock acetabular component. *Int Orthop* 33: 911–916.
15. Macheras GA, Papagelopoulos PJ, Kateros K, et al. (2006) Radiological evaluation of the metal-bone interface of a porous tantalum monoblock acetabular component. *Bone Joint J* 88: 304–309.

16. Gruen TA, Poggie RA, Lewallen DG, et al. (2005) Radiographic evaluation of a monoblock acetabular component: a multilayer study with 2- to 5-year results. *J Arthroplasty* 20: 369–378.
17. D'Angelo F, Murena L, Campagnolo M, et al. (2008) Analysis of bone ingrowth on a tantalum cup. *Indian J Orthop* 42: 275–278.
18. Hanzlik JA, Day JS (2013) Bone ingrowth in well-fixed porous tantalum implants. *J Arthroplasty* 28: 922–927.
19. Hanzlik JA, Day JS, Rimnac CM, et al. (2015) Is there a difference in bone ingrowth in modular versus monoblock porous tantalum tibial trays? *J Arthroplasty* 30: 1073–1078.
20. Levine BR, Sporer S, Poggie RA, et al. (2006) Experimental and clinical performance of porous tantalum in orthopedic surgery. *Biomaterials* 27: 4671–4681.
21. Paganias CG, Tsakotos GA, Koutsostahis SD, et al. (2012) Osseous integration in porous tantalum implants. *Indian J Orthop* 46: 505–513.
22. Paganias CG, Tsakotos GA, Koutsostahis SD, et al. (2014) The process of porous tantalum implants osseous integration: a review. *Am Med J* 5: 63–72.

AIMS Press